



ELSEVIER

Journal of Chromatography A, 975 (2002) 175–188

---

---

JOURNAL OF  
CHROMATOGRAPHY A

---

---

www.elsevier.com/locate/chroma

## Thermodynamic and kinetic models for the extraction of essential oil from savory and polycyclic aromatic hydrocarbons from soil with hot (subcritical) water and supercritical CO<sub>2</sub>

Alena Kubátová, Boris Jansen<sup>1</sup>, Jean-François Vaudoisot, Steven B. Hawthorne\*

Energy and Environmental Research Center, Campus Box 9018, University of North Dakota, Grand Forks, ND 58202, USA

---

### Abstract

Mechanisms that control the extraction rates of essential oil from savory (*Satureja hortensis*) and polycyclic aromatic hydrocarbons (PAHs) from historically-contaminated soil with hot water and supercritical carbon dioxide were studied. The extraction curves at different solvent flow-rates were used to determine whether the extractions were limited primarily by the near equilibrium partitioning of the analyte between the matrix and solvent (i.e. partitioning thermodynamics, or the “elution” step) or by the rate of analyte desorption from the matrix (i.e. kinetics, or the “initial desorption” step). Two simple models were applied to describe the extraction profiles obtained with hot water and with supercritical CO<sub>2</sub>: (1) a model based solely on the thermodynamic distribution coefficient  $K_D$ , which assumes that analyte desorption from the matrix is rapid compared to elution, and (2) a two-site kinetic model which assumes that the extraction rate is limited by the analyte desorption rate from the matrix, and is not limited by the thermodynamic ( $K_D$ ) partitioning that occurs during elution. For hot water extraction, the thermodynamic elution of analytes from the matrix was the prevailing mechanism as evidenced by the fact that extraction rates increased proportionally with the hot water flow-rate. This was also confirmed by the fact that simple removal calculations based on a single  $K_D$  (for each essential oil compound) gave good fits to experimental data for flow-rates from 0.25 to 4 ml/min. In contrast, supercritical CO<sub>2</sub> extraction showed only minimal dependence on flow-rate, and the simple  $K_D$  model could only describe the initial 20–50% of the extraction. However, a simple two-site kinetic model gave a good fit for all CO<sub>2</sub> flow-rates tested. The results of these investigations demonstrated that very simple models can be used to determine and describe extractions which are limited primarily by partitioning thermodynamics, or primarily by desorption kinetics. Furthermore, these results show that the time required for the recovery of essential oil from savory with hot water can be minimized by increasing flow-rate, with little change in the total volume of water required. In contrast, raising the flow-rate of supercritical CO<sub>2</sub> has little effect on the mass of essential oils recovered per unit of time, indicating that optimal recovery of these compounds with supercritical CO<sub>2</sub> (amount recovered for the lowest amount of CO<sub>2</sub>) requires longer extraction times rather than faster flow-rates.

© 2002 Elsevier Science B.V. All rights reserved.

**Keywords:** Essential oils; Savory; Hot water extraction; Supercritical fluid extraction; Polycyclic aromatic hydrocarbons; Carbon dioxide; Water

---

\*Corresponding author.

E-mail address: [shawthorne@undeerc.org](mailto:shawthorne@undeerc.org) (S.B. Hawthorne).

<sup>1</sup>Present address: IBED-Physical Geography, Universiteit van Amsterdam, Nieuwe Achtergracht 166, 1018 WV Amsterdam, The Netherlands.

0021-9673/02/\$ – see front matter © 2002 Elsevier Science B.V. All rights reserved.

PII: S0021-9673(02)01329-8

## 1. Introduction

The desire to obtain faster extractions with environmentally-friendly solvents has led to a great deal of work with supercritical CO<sub>2</sub>, and more recently with hot (subcritical) water. Both solvents have been applied to a wide range of biological and environmental samples, but little effort has been spent on understanding the fundamentals of the extraction process. Even though it is obvious that both the thermodynamics and kinetics of the extraction process must be favorable, the majority of modeling studies focus only on one of those factors. Investigating these extraction mechanisms should not be viewed as an academic exercise, since even a minimal understanding on the relative importance of thermodynamics and kinetics on extraction rates can help greatly with optimizing extraction conditions.

The extraction of any compound from a solid matrix requires two steps. First, the compound must be desorbed from its original binding site in (or on) the sample matrix (generally modeled by rate processes such as diffusion [1–12]), then the compound must be eluted from the sample in a manner analogous to frontal elution chromatography (controlled by the thermodynamic partitioning coefficient,  $K_D$ ) [12–17]. For the purposes of this study,  $K_D$  is defined as the equilibrium concentration in the solid (stationary phase) divided by the concentration in the extraction fluid (mobile phase). In systems where the extraction fluid is saturated, such as the extraction of fat from potato chips or extraction of triglycerides from soybean meal, simple saturation solubility calculations can be used to predict extraction rates [9,16,17]. However, in systems where the bulk solubility of the analyte is sufficient for the extraction to occur, analyte solubility largely affects the extraction rate by its effect on  $K_D$ . In such cases, either the desorption or elution steps (or a combination of both steps) may limit extraction rates [9].

Depending on the extraction conditions and sample matrix, either the rate of the initial desorption step or the elution step can control the actual extraction rates [9]. Several studies have focused on explaining and modeling release mechanisms of a supercritical extraction using carbon dioxide (SFE) [1–18]. For SFE, the contribution of the desorption step is usually (but not always) predominant [1–

12,18–20]. Therefore, kinetic models describing the rates of the desorption step such as the diffusion-based “hot-ball” model [1,2] and simple two-site (or more sites) kinetic models [10,18] have been used to describe the supercritical extraction process. In contrast to SFE, the accelerated solvent extraction with toluene of polychlorodibenzo-*p*-dioxins from fly ash was modeled based only on the thermodynamic partition coefficient ( $K_D$ ), and no kinetic factors were needed to model the results [13]. Similarly, supercritical fluid extraction with CO<sub>2</sub> of the total lipid mass from fat and soybean matrices showed good agreement with predictions based on solubility [16,17]. These results indicate that the mechanism that controls extraction can change based on the extraction fluid employed and/or matrix extracted.

It can be difficult to determine the relative importance of desorption kinetics and thermodynamic partitioning during the elution step by only observing the shape of the extraction curve, since it is possible for both kinetic and thermodynamic models to give good agreement with the experimental data. However, observing the effect of extraction fluid flow-rate on the extraction rates can be a simple approach to determining the relative importance of the two steps. Simply stated, if an extraction is limited by the kinetics of the initial desorption step as described by various kinetic models for SFE [1–11], then doubling the extraction fluid flow-rate should have little effect on the actual extraction rate (versus time) of the target compound. Similarly, if doubling the extraction fluid flow-rate doubles the extraction rate of the desired compound, then the partitioning thermodynamics ( $K_D$ ) limits the extraction rate [9,13–17].

The purpose of this paper is to investigate the mechanisms controlling the extraction rates achieved with two different extraction solvents, hot water and supercritical carbon dioxide. These investigations were performed using samples typical of plant tissue (the extraction of essential oil from savory (*Satureja hortensis*) and environmental samples (the extraction of PAHs from historically-contaminated soil). The relative importance of the desorption (kinetic) step and the elution (thermodynamic) step were determined with both fluids by varying the extraction fluid flow-rate. Two simple models were employed to describe the data. One model attempts to predict the

extraction rates based on the thermodynamic distribution coefficient ( $K_D$ ), and the other model tries to predict the extraction rates using a fast ( $k_1$ ) and a slow ( $k_2$ ) kinetic rate constant.

## 2. Materials and methods

Summer savory (*Satureja hortensis*) obtained from Penn Herb (Philadelphia, PA, USA), was used as received (air dried and coarsely ground). Sample sizes were approximately 1.0 g for each extraction method. After every extraction, the extraction efficiencies of each method were confirmed by extracting the plant tissue residues using 18 h of sonication in 15 ml of acetone. Individual compounds ranged from ~300 to 1200 mg/kg [21].

The PAH-contaminated soil was obtained from a manufactured gas plant (MGP) site, which had been abandoned for several decades and treated for 1 year by bioremediation [18,22]. Individual PAH concentrations ranged from ~5 to 80 mg/kg with a total PAH concentration of 520 mg/kg. The samples were used as received (air dried). Approximately 2 g of soil were used for hot water and supercritical CO<sub>2</sub> extractions. After every extraction, the extraction efficiencies of each method were confirmed by 18 h Soxhlet extraction of soil residues with 150 ml of a methylene chloride–acetone (2:1, v/v).

### 2.1. Hot water extraction

Extraction conditions were chosen to yield a moderate extraction rate for both the essential oils from savory (100 °C and ~60–70 bar) and the PAHs from soil (175 °C and 50 bar) so that any changes which might occur with different flow-rates could be observed [21]. Hot water extraction was performed in a laboratory-built apparatus previously described in detail [23,24]. In brief, the extraction system consists of two ISCO model 100D syringe pumps (ISCO, Lincoln, NE, USA) delivering water and methylene chloride at a constant flow-rate to an HP 5890 gas chromatograph oven (Hewlett-Packard, Wilmington, DE, USA), where the extraction cell was mounted. The water (HPLC grade, Fisher Scientific, Pittsburgh, PA, USA), was purged with nitrogen to remove dissolved oxygen prior to the

extraction, and supplied to the system with the pump at a constant flow of 0.25, 0.5, 1, 2 and 4 ml/min. A second pump delivered methylene chloride at a flow of 1 ml/min to a mixing tee installed in the oven after the outlet of the extraction cell to collect the extracted compounds as the water cooled after exiting the extraction oven. Finally, a miniature back-pressure regulator (Upchurch Scientific, Oak Harbor, WA, USA) was placed at the outlet of the extraction system (outside of the oven) to maintain the system pressure, thus ensuring that the water was in the liquid state at all temperatures tested.

All water extractions of savory were carried out in a 3.47-ml SFE cell (50×9.4 mm I.D., Keystone Scientific, Bellefonte, PA, USA) equipped with a 0.5- $\mu$ m frit at the inlet, and a 2- $\mu$ m frit at the outlet. The larger pore frit was installed at the outlet to prevent plugging with matrix material. In addition, seven layers of glass microfiber filter (1  $\mu$ m, Whatman, Maidstone, UK) were placed inside of the cell to protect the outlet frit. The extraction cell was completely filled with savory (~1.0 g) and mounted vertically in the oven with water flowing from top to bottom. The extractions of PAHs were performed in a 2 ml SFE cell (30×9.4 mm I.D., Keystone Scientific) equipped with 0.2- $\mu$ m frits. To prevent plugging, one layer of filter paper and 0.5 g of sea sand (Fisher) was added at the outlet of the cell.

The extraction procedure started by pressurizing the system with water to ~60 bar at a flow of 1 ml/min (for PAHs the system was pressurized to 50 bar at a flow of 0.5 ml/min) and heating the oven to the required temperature, a process that required 3–5 min. At this time, the back-pressure regulator (set to 60 bar) opened, the water flow-rate was set to the desired rate, the methylene chloride collection solvent flow was started, and collection of the eluent began (extraction time=0). For the extraction rate experiments, the collection vial was replaced at frequent time intervals. For savory, the single sequential experiment for each flow-rate was normalized to the triplicate experiments stopped at 80 min for flow-rates of 0.25 and 5 ml/min, and at 40 min for 1 and 2 ml/min. After each extraction, the methylene chloride fraction was collected and the water fraction rinsed once more with an additional aliquot of methylene chloride. The methylene chloride fractions were analyzed to determine extraction

efficiencies. Since a system void volume of  $\sim 1.25$  ml existed between the extraction cell and collection vessel, hot water extraction curves were time adjusted, e.g. by 5 min (for the 0.25 ml/min flow) and 0.6 min (for the 2 ml/min flow).

## 2.2. Supercritical $CO_2$ extraction

As for the hot water extractions, the experimental conditions selected for SFE were chosen to give moderate extraction rates to allow for better comparison of the extraction curves. For savory, extractions were performed at 50 °C and 400 bar [21,25]. For the PAH-contaminated soil, extractions were performed at 50 °C and 200 bar [18]. SFE was performed using SFE-grade  $CO_2$  (with helium headspace, Scott Specialty Gases, Plumsteadville, PA, USA) supplied to an ISCO SFX 210 extraction unit with a model 260D syringe pump (ISCO). All extractions were performed using the 10-ml cells supplied with the unit. SFE flow-rates were maintained at  $\sim 0.25$ , 1 and 2 ml/min (measured as liquid  $CO_2$  at the pump) using a variable flow restrictor (ISCO) heated to 80 °C. Extracted analytes were collected in 15 ml methylene chloride placed in a 22-ml glass screw-top vial. For the extraction rate experiments, the collection vial was replaced at frequent time intervals. For savory, the single sequential experiment for each flow-rate was normalized to the triplicate experiments stopped at 120 min. For PAHs, the single sequential experiment for each flow-rate was normalized to the triplicate experiments stopped at 80 min.

## 2.3. Gas chromatographic analysis

Quantitative analyses of savory essential oil compounds were performed using GC with flame ionization detection (GC–FID) on a Hewlett-Packard model 5890 Series II gas chromatograph equipped with an autosampler. Chromatographic separations were accomplished with a 30 m DB-5 column with a 0.25 mm I.D. and a 0.25  $\mu$ m film thickness (J&W Scientific, Rancho Cordova, CA, USA) with injections in the splitless mode (0.2 min). The oven temperature was held at 35 °C for 0.2 min and was then increased to 60 °C with a gradient of 30 °C/min, followed by 6 °C/min to 200 °C and then by 30 °C/

min to the final temperature of 320 °C. Quantitations were based on the addition of *n*-dodecane as the internal standard to each extract and on standard calibration curves generated from pure standard compounds.

PAH analyses were also performed on a GC–FID equipped with a 25 m HP-5 column with a 0.25 mm I.D. and a 0.17  $\mu$ m film thickness (Hewlett-Packard) with injections in the splitless mode (0.2 min). The oven temperature was held at 70 °C for 1 min and was then heated with a gradient of 6 °C/min to the final temperature of 320 °C and held for 2 min. The internal standard was 1-chloronaphthalene. All essential oil compound and PAH identifications, and the lack of other interfering hydrocarbons for both savory essential oil and PAH analyses were confirmed by GC–MS using the same chromatographic conditions.

## 2.4. Data analysis

The simple thermodynamic model is based on a single distribution coefficient defined as  $K_D = (\text{concentration of analyte in the matrix}) \div (\text{concentration of analyte in the extraction fluid})$  at equilibrium [13]. For this model, it is assumed that the kinetics of the initial desorption step and subsequent fluid–matrix partitioning are rapid, and thus do not significantly affect the extraction rate. Essentially, the mass of analyte in each unit mass of extraction fluid and the mass of analyte remaining in the matrix at that period in the extraction time is calculated for the entire extraction time based on the  $K_D$  value determined for each compound. Therefore, if the  $K_D$  model applies to a certain extraction, the shape of an extraction curve would be defined by:

$$\frac{S_b}{S_0} = \left(1 - \frac{S_a}{S_0}\right) \div \left(\frac{K_D m}{(V_b - V_a)d} + 1\right) + \frac{S_a}{S_0} \quad (1)$$

where  $S_a$  is the cumulative mass of the analyte extracted after volume  $V_a$  (ml), and  $S_b$  is the cumulative mass of the analyte extracted after volume  $V_b$  (where the data point  $V_b$ ,  $S_b$  is the next sequential data point after  $V_a$ ,  $S_a$ ).  $S_0$  is the initial total mass of analyte in the matrix.  $S_b/S_0$  and  $S_a/S_0$  are the cumulative fractions of the analyte extracted by the extraction fluid of the volume  $V_b$  and  $V_a$ , respectively.

$K_D$  is the distribution coefficient,  $d$  is the density of extraction fluid at given conditions (g/ml), and  $m$  is the mass of the extracted sample (g). The Microsoft EXCEL Solver regression routine was used to fit extraction data to Eq. (1). The parameter of fit was  $K_D$ . Note that the  $K_D$  model does not include extraction time, but only relies on the volume of extractant fluid used (assuming a constant sample size). Therefore, doubling the extraction fluid flow-rate should double the extraction rate versus time if the extraction is described by thermodynamic partitioning (and if all other extraction parameters remain the same).

Kinetic desorption models typically require two steps to define an extraction curve, i.e. a certain fraction ( $F$ ) of the analytes desorb at a fast rate defined by  $k_1$ , and the remaining fraction ( $1 - F$ ) desorbs by a slower rate defined by  $k_2$  [18,22]. The simple two-site kinetic model consists of two first-order expressions [18]:

$$\frac{S_t}{S_0} = 1 - [F e^{-k_1 t}] - [(1 - F) e^{-k_2 t}] \quad (2)$$

where  $t$  is time (min),  $S_t$  is the mass of the analyte removed by the extraction fluid after time  $t$ ,  $S_0$  is the total initial mass of analyte in the matrix.  $S_t/S_0$  is the fraction of the analyte extracted after the time  $t$ ,  $F$  is the fraction of the analyte released quickly,  $(1 - F)$  is the fraction of the analyte released slowly;  $k_1$  is the first-order rate constant describing the quickly released fraction ( $\text{min}^{-1}$ ); and  $k_2$  is the first-order rate constant describing the slowly released fraction ( $\text{min}^{-1}$ ). Note that the kinetic model includes no factor describing extraction flow-rate, but relies solely on time. Therefore, doubling the extractant flow-rate should have little effect on the extraction efficiency per unit time if the extraction efficiency is controlled by the kinetics of the initial desorption step (assuming the other extraction parameters remain constant). The Microsoft EXCEL Solver regression routine was used to fit release data to Eq. (2). The parameters of fit were  $F$ ,  $k_1$ , and  $k_2$  as previously described [18,22].

While it is possible that a single-site kinetic model and a  $K_D$  model could yield similar fits to extraction curve data, the dependence of the  $K_D$  model on extraction fluid volume (not time) and the dependence of kinetic models on extraction time (not

volume of fluid) yields a simple method to determine the major factor controlling a particular extraction.

### 3. Results and discussion

Fig. 1 shows extraction curves generated from SFE and hot water extraction of representative savory compounds and PAHs from soil (all at a flow of 1 ml/min). The general shape of these curves are fairly typical of extraction rate curves shown in the literature [1–15,17–21,25–28], i.e. SFE typically (but not always) shows an initial extraction phase which is substantially faster than a subsequent slow phase. In contrast, hot water extraction typically shows little drop in extraction rates until the target analyte is nearly depleted from the matrix. While it is tempting, based on these plots, to assign the thermodynamic  $K_D$  model to the hot water extractions, and the two-site kinetic model to the SFE curves, we cannot make that interpretation based only on the results in Fig. 1. The reason is that, without knowledge of the effect of flow-rate, the relative importance of the desorption kinetics and the extraction curves for hot water could be described by a single site kinetic model, as well as the single  $K_D$  model proposed above. Similarly, the SFE curves could be described by a two-site thermodynamic model (i.e. if the matrix had two types of sorption sites, one with a lower  $K_D$  and one with a higher  $K_D$ ), as well as the two-site kinetic model proposed above.

#### 3.1. Effect of flow-rate

Based on the discussion above, the importance of  $K_D$  and desorption kinetics was determined by comparing the effects of changing flow-rate on the extraction rate of the same samples (Fig. 2). Note that with hot water, the extraction rates of the essential oil showed an increase in extraction rate that was proportional to the extraction fluid flow-rate regardless of whether the compound was extracted rapidly (e.g. thymol) or slowly (e.g. *p*-cymene). The hot water curves all show the behavior expected based on the  $K_D$  model equation (above), i.e. direct dependence of extraction rate on flow-rate and near linear extraction curves until the target compounds are nearly depleted from the matrix.

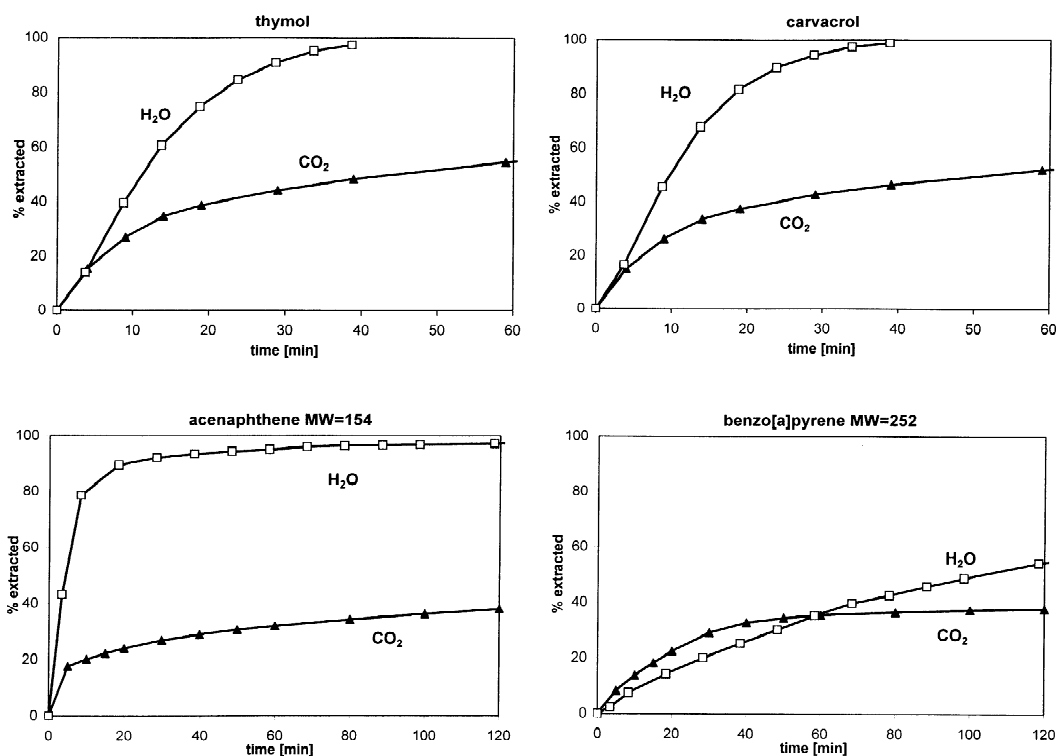


Fig. 1. Comparison of hot water and supercritical CO<sub>2</sub> extraction profiles for representative essential oil compounds from savory (top) and PAHs from contaminated soil (bottom).

In contrast, the extraction curves for SFE only show a change in extraction rate during the initial (~20–30% extracted) portion of the curve, and mostly when the flow-rate was increased from 0.25 to 1 ml/min. At flow-rates more typically used for SFE (1 and 2 ml/min), there was only small differences in the extraction rates. This demonstrates that the SFE process was controlled primarily by kinetics of the desorption process for both essential oil compounds from savory. (Flow-rates higher than 2 ml/min were not tested for SFE, because of less than quantitative collection efficiencies for the more volatile compounds.)

Note that in addition to the flow-rate behavior, other features expected for the two-site kinetic model are observed for SFE curves, regardless of the compound being extracted. That is, after the initial fast fraction is removed (~20–30% extracted), the portion of the curves controlled by the slow desorption rate become increasingly parallel, regardless of flow-rate.

### 3.2. Model based on the distribution coefficient, $K_D$

The effect of different values of the thermodynamic distribution coefficient ( $K_D$ ) on extraction rates (with a constant flow-rate of 1 ml/min) is shown in Fig. 3. As expected, a higher  $K_D$  (stronger competition of the matrix versus the fluid for the solute) yields slower extraction rates. Based on a comparison of Fig. 3 with the experimental data shown in Figs. 1 and 2, it appears that the  $K_D$  model shows the general extraction curve shape behavior typical of hot water extraction, regardless of whether the compound is extracted rapidly (e.g. thymol) or slowly (e.g. *p*-cymene). In addition, visual comparisons of Figs. 2 and 3 indicates that the compounds extracted by hot water have a range of  $K_D$  values from ~10 (oxygenated essential oil compounds such as thymol) to ~100 (e.g. *p*-cymene).

The effects of flow-rate on extraction curves for the representative  $K_D=10$  and  $K_D=100$  are shown

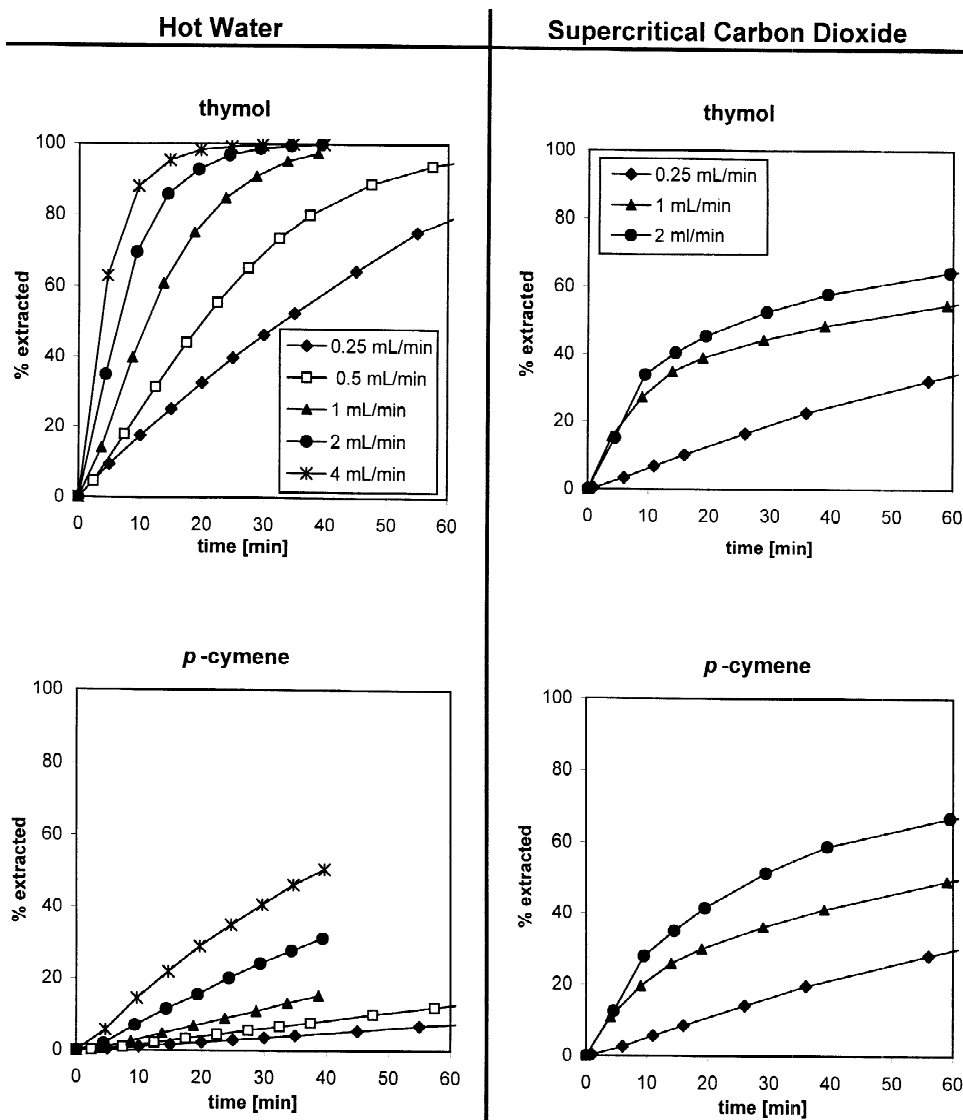


Fig. 2. Effect of extraction fluid flow-rate on hot water and supercritical  $\text{CO}_2$  extraction of thymol and *p*-cymene from savory.

in Fig. 4. Note that the general agreement of the theoretical curves with the experimental curves from the hot water extraction (Fig. 2) is good, but the  $K_D$  theoretical curves do not agree with the SFE curves shown in Fig. 2. It is important to note that the  $x$  axis values are in units of time (not volume). If the same data were plotted in terms of volume, the theoretical curves from all flow-rates would overlap completely, as is required by the  $K_D$  model since no time parameter is included in the calculations.

To further test the  $K_D$  model's ability to match hot water extraction curves,  $K_D$  values were calculated using two methods. First, the slope of the straight initial portion of the extraction curve is proportional to  $K_D$ , and can be most easily measured at the lowest flow-rate. Therefore,  $K_D$  values were calculated by dividing the concentration in the sample matrix after the initial extraction time (i.e. the fraction remaining in the matrix divided by the sample mass) by the average concentration in the extraction fluid passed

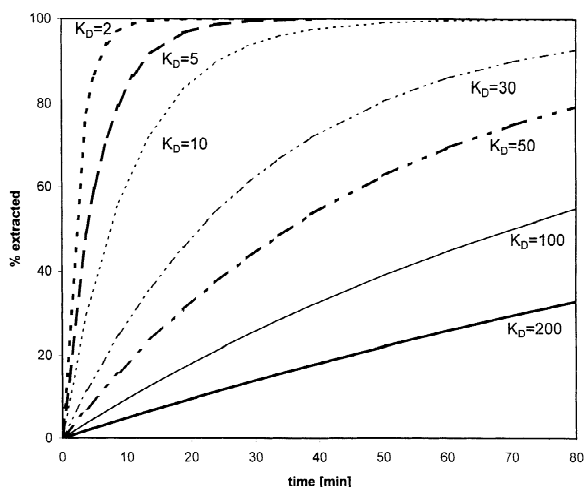


Fig. 3. Theoretical curves calculated using Eq. (1) for extractions controlled by thermodynamic partitioning at a flow of 1 ml/min.

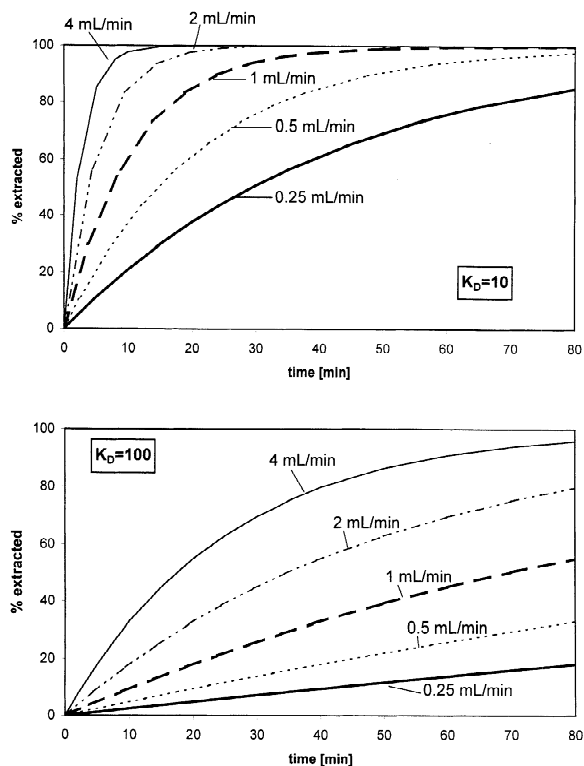


Fig. 4. Theoretical extraction curves for  $K_D$  values of 10 and 100 for extractions controlled by thermodynamic partitioning at flow-rates of 0.25, 0.5, 1, 2 and 4 ml/min.

through the sample during the same initial extraction time (i.e. the fraction extracted divided by the water mass). Second, the model Eq. (1) (above) and the experimental data from all flow-rate plots were used to determine the  $K_D$  value by minimizing the errors between the measured data and the  $K_D$  model data results.

As shown in Table 1, the  $K_D$  values obtained with the two methods (at 0.25 ml/min) agreed well, and demonstrated that individual essential oil compounds have a range of  $K_D$  values from  $\sim 4$  to  $\sim 250$ . The variations in  $K_D$  values shown in Table 1 (for different flow-rates) for a single compound have little effect on the calculated extraction curve, as shown in Figs. 3 and 4. For example, in Fig. 5 the calculated  $K_D$  values determined at 0.25 ml/min for thymol ( $K_D=12$ ) and *p*-cymene ( $K_D=215$ ) were used to calculate the model curves for all flow-rates. As shown in Fig. 5, the use of the single  $K_D$  value yielded model extraction curves which agree well with the experimental data at all flow-rates. In addition, when the  $K_D$  model was applied to the hot water extraction of PAHs from the contaminated soil, the calculated extraction curve and the experimental curves also show good agreement as shown in Fig. 6.

Although all of the compounds extracted from savory with water agreed with the  $K_D$  model, the most striking example is *p*-cymene since its extraction rates are slow enough that the extraction curves are near linear at all flow-rates. As shown in Fig. 5, each increase in flow-rate brought a proportional increase in extraction rate for *p*-cymene, and model curves based on the  $K_D$  determined from the 0.25 ml/min data gave good agreement with the experimental curves at all flow-rates.

Based on the results shown in Fig. 5, it could be objected that the recovery of *p*-cymene is controlled by saturation of the water during the extraction, rather than by near-equilibrium partitioning between the sample matrix and the water during the extraction. However, as discussed above, we ensured that all analytes reported in this work were below saturation conditions, both in the hot water and in the supercritical  $\text{CO}_2$ . The compound *p*-cymene has the lowest solubility in water of all compounds extracted from savory, i.e. 80  $\mu\text{g}/\text{ml}$  at the conditions used for savory extraction [29]. Since the concentration of *p*-cymene in this savory sample is  $550 \pm 3 \mu\text{g}/\text{g}$  [21], saturation of the water with *p*-cymene would yield a



Table 1  
 $K_D$  values for the hot water extraction of savory

Flow (ml/min)	$K_D$					
	Measured <sup>a</sup>	Model curve fitting <sup>b</sup>				
	0.25	0.25	0.5	1.0	2.0	4.0
Thymol	12	12	12	11	12	11
Carvacrol	11	10	11	10	10	9
Borneol	9	7	7	7	8	– <sup>c</sup>
Thymoquinone	4	3	3	3	3	–
<i>p</i> -Cymene	230	215	230	240	222	228

<sup>a</sup> Measured  $K_D$  values were calculated based on the initial slope of the extraction curves obtained at 0.25 ml/min.

<sup>b</sup> Model curve fitting  $K_D$  values were based on fitting the experimental data with Eq. (1).

<sup>c</sup> No  $K_D$  value was determined because the extraction rate was too fast to obtain multiple data points before 100% extraction.

slope of 14% extracted per ml of water. As shown in Fig. 5, the maximum slope of the *p*-cymene curves is <1% extracted per ml of water (or <~5 µg *p*-cymene per ml) which is substantially below the saturation point.

Similarly, the PAHs extracted from soil (Fig. 6) were not limited by saturation in the hot water. For example, the least soluble PAH shown in Fig. 6, benzo[*a*]pyrene has a concentration of 40 µg/g in the soil which would result in 80 µg of benzo[*a*]pyrene from the 2-g soil sample. As shown in Fig. 6, the maximum concentration found in the water is ~10% (or 8 µg) of the benzo[*a*]pyrene in the first 10 ml of water, which corresponds to a maximum concentration in water of <1 µg/ml. This concentration is considerably below the solubility limit of ~45 µg/ml (estimated from the solubility data in Ref. [24]).

Finally, the  $K_D$  model was applied to the SFE extraction curves by calculating the  $K_D$  value of each compound based on the initial linear portion of the extraction curve generated at the slowest flow-rate as described above. As shown in Fig. 7, the model curves generated from the  $K_D$  values calculated from the 0.25 ml/min plots (up to 120 min) fail to predict the behavior obtained at higher flow-rates, thus proving that the elution step (or thermodynamic partitioning) does not control the supercritical CO<sub>2</sub> extraction of essential oil compounds from savory. Similar behavior was observed for PAHs.

### 3.3. Two-site kinetic model

Because the model based on the distribution coefficient,  $K_D$ , was not suitable for the description

of SFE, the two-site kinetic model described above was tested by curve fitting the savory extraction data using the fast fraction (*F*), the fast desorption rate constant ( $k_1$ ) and the slow rate constant ( $k_2$ ) as previously described for the SFE of PAHs from soil [18].

Only a single rate constant is required to describe the curves for the extraction of savory at the lowest flow-rate (0.25 ml/min) since the extraction efficiencies (and extraction times) were not high enough to see both “fast” and “slow” parts of the curve (Fig. 8). Thus, a single rate constant was sufficient to describe the 0.25 ml/min curves. (As noted above, it is also possible that the 0.25 ml/min curve from 0 to ~50% extracted is controlled by  $K_D$ , rather than  $k_1$ , but  $K_D$  control does not explain the extraction curves at the higher flow-rates.) However, the two-site kinetic model applies well to the higher flow-rates as shown in Fig. 8, compared to the failure of the  $K_D$  model shown in Fig. 7.

Inspection of the 1 and 2 ml/min flow-rate data in Fig. 8 demonstrates that the extraction rates are not completely independent of flow-rate. As discussed above, demonstrating that desorption kinetics have no significant effect on extraction rates is straightforward using the flow-rate experiments for extractions controlled by the  $K_D$  mechanism. However, while the  $K_D$  model depends directly on the extraction flow-rate (at a constant sample size), the actual processes controlling extraction rates are not totally independent of the flow-rate for samples controlled by desorption kinetics. Since the driving force of the desorption from the matrix into the fluid is the concentration gradient from the soil to the extraction fluid [1,11], a faster flow-rate will give a

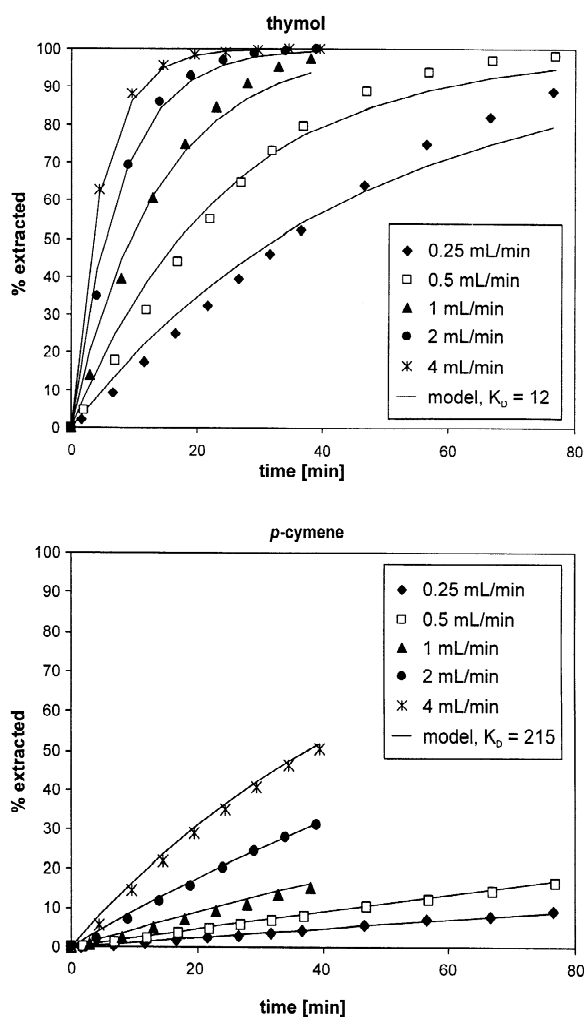


Fig. 5. Comparison of the  $K_D$  model fit with experimental data for the hot water extraction of thymol and *p*-cymene from savory. Symbols represent the experimental data and the solid lines are calculated from Eq. (1) based on the  $K_D$  values obtained at a flow-rate of 0.25 ml/min.

somewhat faster extraction rate, particularly in the early part of the extraction where the analyte concentration is the highest. A second flow-rate influence is that a higher flow-rate will cause a faster elution of more rapidly-desorbed molecules from simple void volume considerations.

Since the two-site kinetic model does not attempt to directly account for flow-rate, these two influences would be expected to result in somewhat higher values of  $F$  when comparing the 2 ml/min to 1

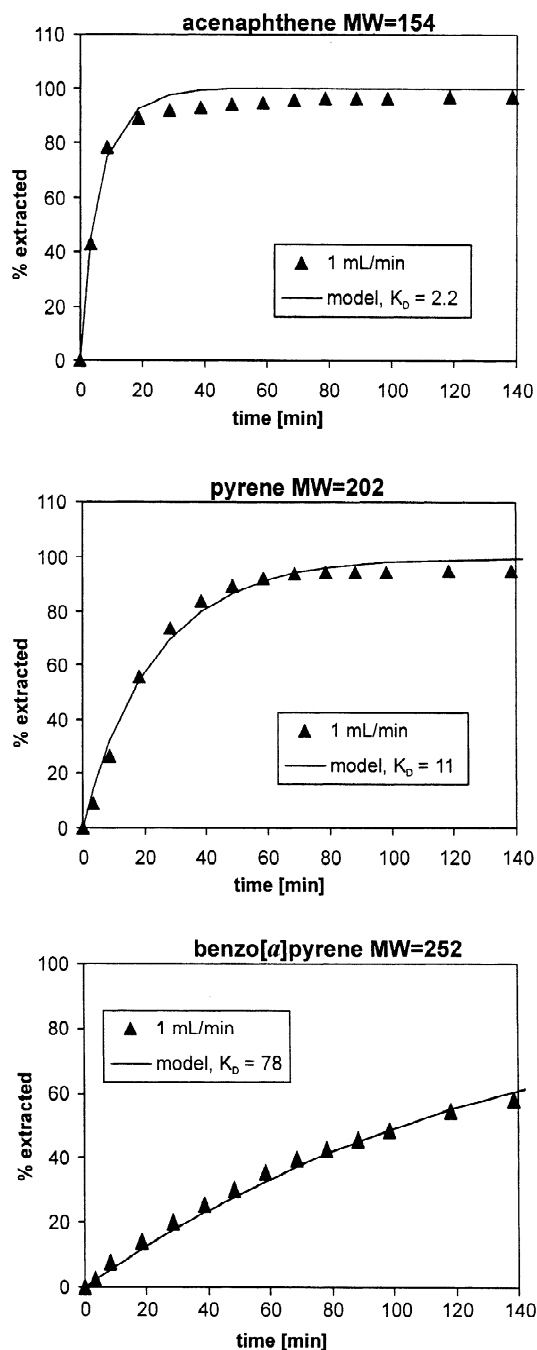


Fig. 6. Comparison of the  $K_D$  model fit with experimental data for the hot water extraction of representative low and high-molecular-mass PAHs from contaminated soil. Symbols represent the experimental data and the solid lines are calculated from Eq. (1) based on the  $K_D$  values obtained by curve fitting the experimental data.

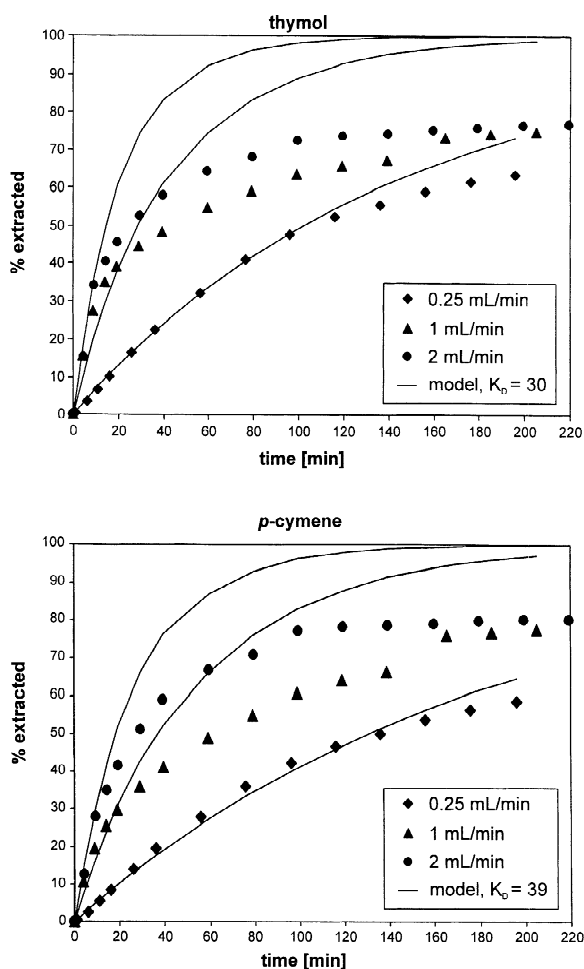


Fig. 7. Failure of the simple  $K_D$  model to fit experimental SFE extraction profiles of essential oil compounds from savory. Symbols represent the experimental data, and the solid lines are calculated from Eq. (1) based on  $K_D$  values calculated from the initial slope of the 0.25 ml/min curves.

ml/min extractions. Similarly, once the “fast” ( $k_1$ ) molecules are depleted (~30–40% extraction efficiency in Fig. 8), the influence of flow-rate should become negligible since the kinetics of desorption ( $k_2$ ) are now very slow compared to flow-rate effects. This would result in the  $k_2$  values being the same for the 2 and 1 ml/min flow-rates. In other words, the extraction curves become parallel after the fast fraction is depleted. Comparison of the  $F$  and  $k_2$  values for all of the compounds studied from savory support this argument, as shown in Table 2.

Table 2

Values of  $F$ ,  $k_1$  and  $k_2$  for SFE of essential oil from savory based on the two-site kinetic model

Flow (ml/min)	$F^a$		$k_1$		$k_2$	
	1.0	2.0	1.0	2.0	1.0	2.0
Thymol	0.37	0.48	0.12	0.09	0.005	0.006
Carvacrol	0.36	0.48	0.12	0.09	0.005	0.005
Borneol	0.25	0.37	0.12	0.07	0.006	0.007
Thymoquinone	0.20	0.53	0.15	0.05	0.011	0.013
<i>p</i> -Cymene	0.26	0.50	0.11	0.06	0.006	0.007

<sup>a</sup> The fast fraction  $F$  and the fast and slow desorption rate constants ( $k_1$  and  $k_2$ ) were obtained by curve fitting the experimental data with Eq. (2).

Similar to the savory results, when the PAH contaminated soil is extracted by supercritical  $\text{CO}_2$ , there is little or no dependence on flow-rate, and the two-site kinetic model must be applied to describe the extraction rates, as shown by the extraction for different PAHs in Fig. 9.

#### 4. Summary and conclusions

Although the kinetics of extraction with hot water have not been studied for a large number of samples, examples in the literature [13,26–28], and the authors' experience indicate that the  $K_D$  model generally appears to fit hot water extractions (although kinetically-limited extractions will almost certainly occur with some samples). Conversely, many of the kinetic curves reported for supercritical  $\text{CO}_2$  appear to have “fast” and “slow” regions consistent with the two-site kinetic model, but some curves consistent with the  $K_D$  model are also reported [1,14–17]. Generally speaking, it appears that supercritical  $\text{CO}_2$  extraction tends to show “fast” and “slow” extraction behavior of compounds which are less-strongly and more-strongly associated with the sample matrix, likely because SFE has less tendency to extract matrix organics than hot water [30]. Thus, SFE with pure  $\text{CO}_2$  can yield information as to the relative “availability” of compounds on a sample matrix. For example, PAHs which extract in the “fast” fraction from historically contaminated soil under mild SFE have been shown to be bioavailable during treatment of contaminated sites, while PAHs

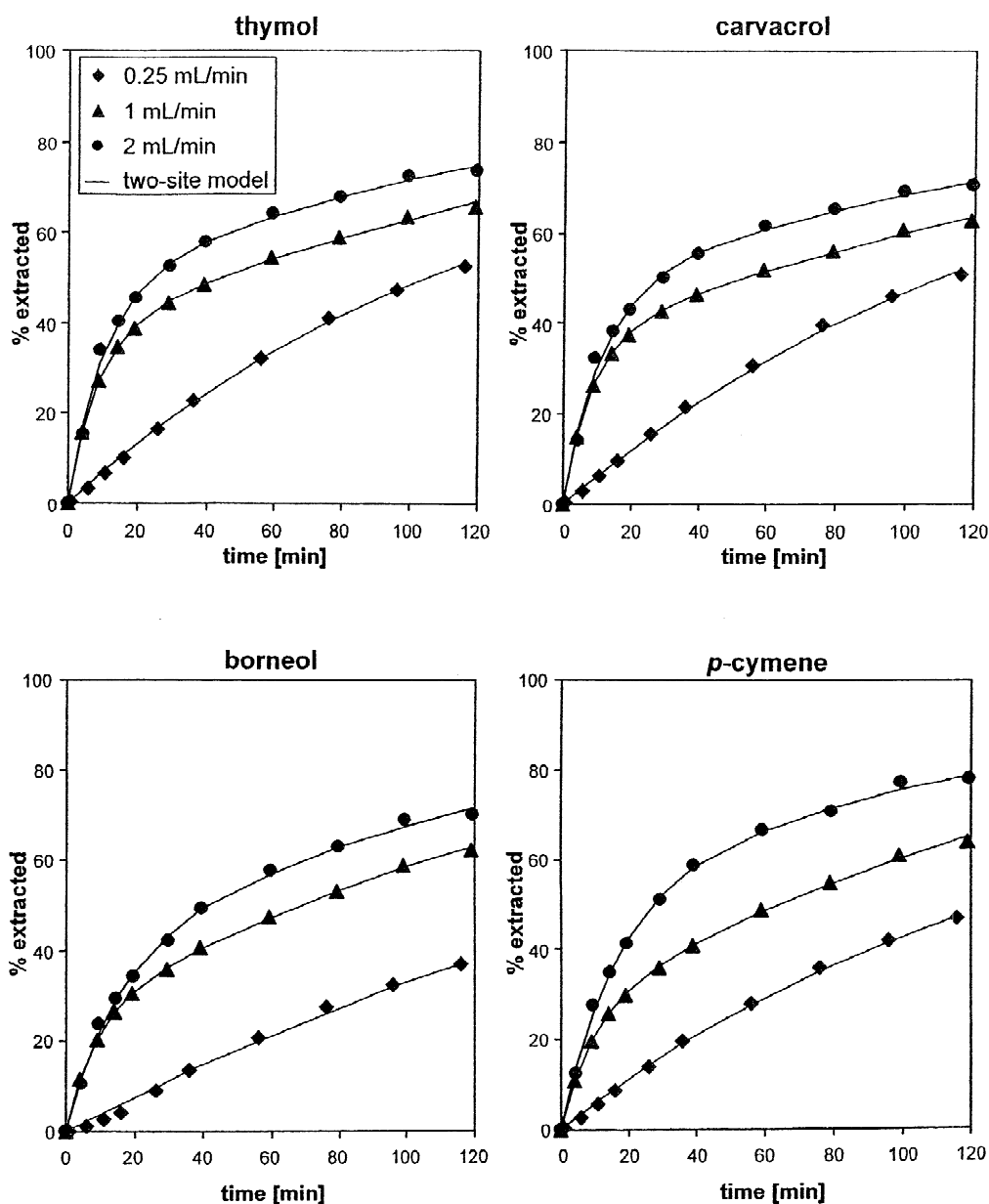


Fig. 8. Two-site kinetic model fit of supercritical  $\text{CO}_2$  extraction data of essential oil compounds from savory. Symbols represent the experimental data, and the solid lines are based on curve fitting the experimental data using Eq. (2) as described in the text.

which are “slow” under the same SFE conditions are not bioavailable [18].

In contrast to SFE, hot water extraction appears to make all analyte binding sites more equivalent as evidenced that the simple  $K_D$  model can describe the extraction behavior. Presumably, hot water is more

effective at altering sample matrices and displacing analytes from their original binding sites than supercritical  $\text{CO}_2$ . Unfortunately, generalizations are difficult to support since there have been few attempts reported in the literature to differentiate the relative influence of elution thermodynamics and the kinetics

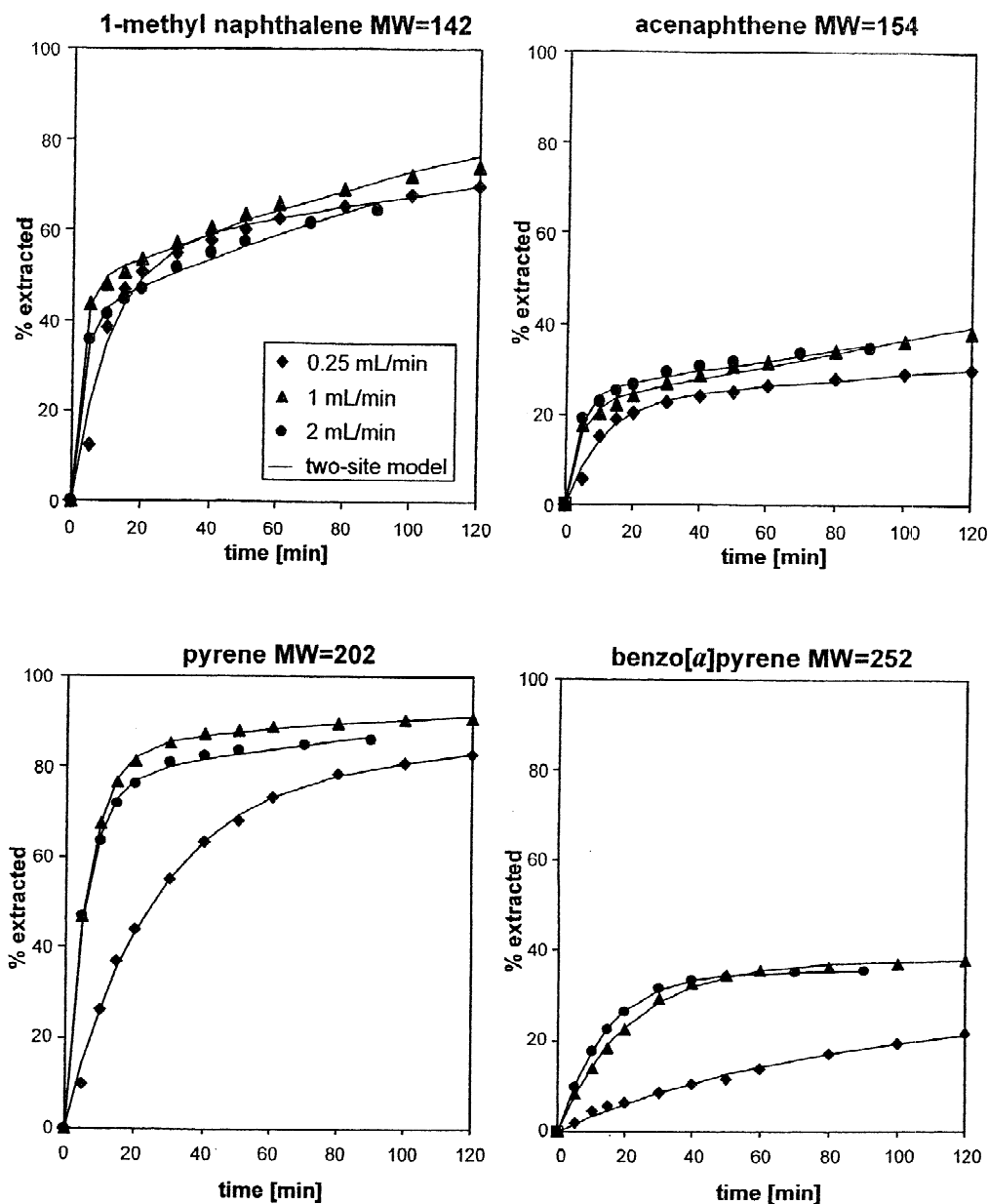


Fig. 9. Two-site kinetic model fit of supercritical  $\text{CO}_2$  extraction data of representative PAHs from contaminated soil. Symbols represent the experimental data, and the solid lines are based on curve fitting the experimental data using Eq. (2) as described in the text.

of desorption on extraction rates and recoveries from real-world samples.

To some readers, modeling of extraction data to provide insights into extraction mechanisms may appear to be only useful for academic purposes. However, the simple flow-rate study discussed above

and the evaluation of simple  $K_D$  and two-site kinetic models can also provide very practical direction on what parameters to address in developing extraction conditions. This can be especially useful when it is important to reduce the volume of extraction solvent. For example, the results shown in Fig. 8 for SFE

demonstrate that using high flow-rates of supercritical CO<sub>2</sub> has little benefit for obtaining higher recoveries of essential oil compounds from savory. Therefore, one must either extract for long periods of time, or change SFE conditions (or modify the matrix, e.g. by grinding) to increase the rate of the slow rate constant ( $k_2$ ) to achieve high recoveries in more reasonable amounts of time. In contrast, hot water extraction of savory (Fig. 5) shows increased recovery rates directly proportional to extraction flow-rates, demonstrating that high water flow-rates can be used to shorten extraction times without increasing the amounts of fluid needed to achieve a high recovery.

## References

- [1] K.D. Bartle, A.A. Clifford, S.B. Hawthorne, J.J. Langenfeld, D.J. Miller, R. Robinson, *J. Supercrit. Fluids* 3 (1990) 143.
- [2] K.D. Bartle, T. Boddington, A.A. Clifford, S.B. Hawthorne, *J. Supercrit. Fluids* 5 (1992) 207.
- [3] E. Reverchon, G. Donsi, L.S. Osséo, *Ind. Eng. Chem. Res.* 32 (1993) 2721.
- [4] M. Goto, B.C. Roy, T. Hirose, *J. Supercrit. Fluids* 9 (1996) 128.
- [5] T. Veress, *J. Chromatogr. A* 668 (1994) 285.
- [6] M.J. Cocero, J. García, *J. Supercrit. Fluids* 20 (2001) 229.
- [7] M.J. Cocero, J. García, *J. Supercrit. Fluids* 20 (2001) 245.
- [8] M. Poletto, E. Reverchon, *Ind. Eng. Chem. Res.* 35 (1996) 3680.
- [9] S.B. Hawthorne, A.B. Galy, V.O. Schmitt, D.J. Miller, *Anal. Chem.* 67 (1995) 2723.
- [10] K. Pilorz, E. Björklund, S. Bøwadt, L. Mathiasson, S.B. Hawthorne, *Environ. Sci. Technol.* 33 (1999) 2204.
- [11] J.J. Langenfeld, S.B. Hawthorne, D.J. Miller, J. Pawliszyn, *Anal. Chem.* 34 (1995) 1727.
- [12] J. Pawliszyn, *J. Chromatogr. Sci.* 31 (1993) 31.
- [13] I. Windal, D.J. Miller, E. de Pauw, S.B. Hawthorne, *Anal. Chem.* 72 (2000) 3916.
- [14] J. Hwang, S.J. Park, M.D. Deo, F.V. Hanson, *Ind. Eng. Chem. Res.* 34 (1995) 1280.
- [15] E. Cassel, J.V. de Oliveira, *J. Supercrit. Fluids* 9 (1996) 6.
- [16] J.W. King, *J. Chromatogr. Sci.* 27 (1989) 355.
- [17] F. Favati, J.W. King, M. Mazzanti, *J. Am. Oil Chem. Soc.* 68 (1991) 422.
- [18] S.B. Hawthorne, D.G. Poppendieck, C.B. Grabanski, R.C. Loehr, *Environ. Sci. Technol.* 35 (2001) 4577.
- [19] E. Björklund, S. Bøwadt, L. Mathiasson, S.B. Hawthorne, *Environ. Sci. Technol.* 33 (1999) 2193.
- [20] S.B. Hawthorne, E. Björklund, S. Bøwadt, L. Mathiasson, *Environ. Sci. Technol.* 33 (1999) 2204.
- [21] A. Kubátová, A.J.M. Lagadec, D.J. Miller, S.B. Hawthorne, *Flavour Fragr. J.* 16 (2001) 64.
- [22] R.C. Loehr, M.T. Webster, *Pract. Period. Hazard., Toxic, Radioact. Waste Manag.* 4 (2000) 53.
- [23] D.J. Miller, S.B. Hawthorne, *J. Chem. Eng. Data* 45 (2000) 315.
- [24] D.J. Miller, S.B. Hawthorne, *Anal. Chem.* 70 (1998) 1618.
- [25] S.B. Hawthorne, M.-L. Riekkola, K. Serenius, Y. Holm, R. Hiltunen, K. Hartonen, *J. Chromatogr.* 634 (1993) 297.
- [26] M.S. Krieger, J.L. Wynn, R.N. Yoder, *J. Chromatogr. A* 897 (2000) 405.
- [27] V. Fernández-Pérez, M.M. Jimenéz-Carmona, M.D. L de Castro, *Analyst* 125 (2000) 481.
- [28] M.M. Jimenéz-Carmona, V. Fernández-Pérez, M.J. Gualda-Bueno, J.M. Cabanás-Espejo, M.D. L de Castro, *Anal. Chim. Acta* 395 (1999) 113.
- [29] D.J. Miller, S.B. Hawthorne, *J. Chem. Eng. Data* 45 (2000) 78.
- [30] S.B. Hawthorne, C.B. Grabanski, E. Martin, D.J. Miller, *J. Chromatogr. A* 892 (2000) 421.